Available online at www.sciencedirect.com
ScienceDirect
Engineering Geology 88 (2006) 121 – 132
ENGINEERING GEOLOGY
www.elsevier.com/locate/enggeo

Numerical analysis of the performance of wire mesh and cable net rockfall protection systems

N. Sasiharan [a], B. Muhunthan [a,*], T.C. Badger [b], S. Shu [a], D.M. Carradine [c]

[a] *Washington State University, Pullman, Washington, USA*
[b] *Washington State Department of Transportation, Tumwater, Washington, USA*
[c] *Wood Materials Engineering Laboratory, Washington State University, Pullman, Washington, USA*

Received 10 November 2005; received in revised form 2 August 2006; accepted 6 September 2006
Available online 25 October 2006

Abstract

Wire mesh and cable net systems have long been used to control rockfall on actively eroding slopes. The design of these systems has been primarily based on empirical methods, engineering judgment, and experience; their performance has been mixed. There is a general consensus among specialists that in wire mesh systems that have functioned well some elements may be over-designed or even unnecessary. On the contrary, system failures under a variety of loading conditions have occurred within the last few decades, indicating that certain design elements may in fact be under-designed for their desired application.

This study presents the results of finite element analyses conducted to examine the performance of the individual elements as well as the overall stability of the wire mesh systems. The load–displacement behaviors of widely used fabrics were determined in the laboratory.

The friction between the mesh and rock can be a major contributor to the stability of the wire mesh and cable net systems. The interface friction is controlled by macro and micro roughness of the surface. Interface friction is a difficult parameter to quantify in practice. Guidelines are provided to estimate this parameter from observed slope irregularity and surface roughness based on finite element analyses.

The top horizontal rope is an essential element in the design of wire mesh and cable mesh systems. The study also shows that the inclusion of interior horizontal support ropes does not reduce the stress within the mesh, and accordingly, provides no mechanical benefit. Results show that the use of vertical ropes eliminates stress concentration around the anchor support and reduces stresses on the top horizontal rope provided that they are clamped to the mesh at closed intervals.

Keywords: Rockfall; Wire mesh; Cable net; Friction; Stability; Finite element analysis

1. Introduction

Rockfall presents a common hazard to transportation routes and structures in steep mountainous terrain. Geology and climate are the principal causal mechanisms of rockfall factors that include intact condition of the rock mass, discontinuities within the rock mass,

* Corresponding author. Department of Civil and Environmental Engineering, Washington State University Pullman, WA 99164 USA. Tel.: +1 509 335 3921; fax: +1 509 335 7632.
E-mail address: muhuntha@wsu.edu (B. Muhunthan).

0013-7952/$ - see front matter © 2006 Elsevier B.V. All rights reserved.
doi:10.1016/j.enggeo.2006.09.005

weathering susceptibility, ground and surface water, freeze–thaw, root-wedging, and external stresses (Smith and Duffy, 1990; Hearn and Akkaraju, 1995; Hearn, 1995). Rockfall initiation and trajectory is a function of slope and rock geometry as well as the slope and rock material properties (Ritchie, 1963; Pfeiffer and Higgins, 1990). Since these are often extremely difficult to predict and quantify, prevention of rockfall is often not viable or cost-effective. Therefore, it is a common practice along highways to provide protection such as ditches, fences, barriers, and wire mesh and cable net protection systems.

Since the1950s, heavy gage wire mesh has been placed directly on the slope surface along North American highways to control rockfall on actively eroding slopes. Within the last fifteen years, small diameter wire rope (cable) nets have been employed as a more robust alternative to wire mesh. With the exception of the anchors and support ropes, the basic design of unsecured systems is comparatively similar throughout North America. It consists of a top horizontal rope suspended by regularly spaced anchors, typically a perimeter or widely spaced grid of support ropes, and double-twisted, hexagonal wire mesh laced to the support ropes (Fig. 1).

The design of these elements has largely been based on empirical guidelines. For example, the Washington State Department of Transportation used the following guidelines until recently:

Fabric

Double twist for block sizes <0.6 m (2 ft)
Cable net for block sizes <9–1.5 m (3–5 ft)
Minimal use of chainlink fabric on flatter slopes

Anchor

15.24 m (50 ft) anchor spacing for slopes <22.86 m (75 ft) high
7.62 m (25 ft) anchor spacing for slopes >22.86 m (75 ft) high
Locate anchors 3–10 m (10–30 ft) beyond active brow
No mid slope anchors

Similar guidelines are followed by other states in the United States and Canada. There is, however, a conflicting opinion on the safety of such elements in practice. While certain states have determined the current empirical guidelines to be safe and conservative, other states such as Washington have experienced failure of individual, or a combination of all of the three main elements. The failure has been in the form of pullout of anchors (Fig. 2a), tear and rupture of the fabric due to large concentrated static load consisting of pockets of rock and/or snow (Fig. 2b and c, and puncture of the fabric due to rock impact (Fig. 2d).

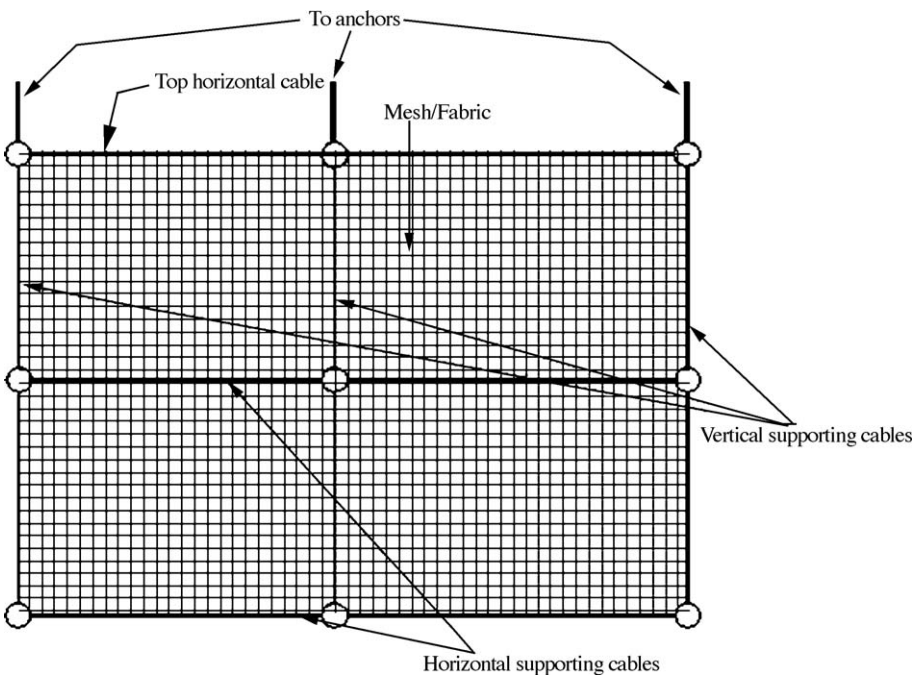

Fig.1. Schematic drawing shows basic elements of a drape mesh system.

Snow loading has also contributed to an increase in the incidence of such failures in some states. It is understood that most of the failure due to the rupture of the fabric has been towards the bottom of the mesh. This may be due to the accumulation of debris at the foot of the slope, and the transmission of considerable impact energy from falling rocks, or a combination of both. There is little information on what influence these concentrated or external loads have on these slope protection systems. To the authors' knowledge there is only one study by the Ministry of British Columbia that evaluated drapery mesh system performance experimentally and numerically (Sandwell Incorporated, 1995).

This paper presents the results of numerical analyses conducted to examine the performance of some of the key elements of the wire mesh and cable net systems. It focuses on the effect of mesh weight, the interface friction between mesh and rock surfaces, and the accumulation of debris on the overall stability of the systems.

2. Fabric properties

Current practice for transportation applications in North America has generally utilized two types of fabric for draped rockfall protection systems; hexagonal wire mesh and woven cable nets with pressed cross clips. Within the last several years, high tensile steel wire mesh (TECCO®) has been introduced in North America. Each of these fabric types has distinctly different weight, strength and elongation properties. Unfortunately, very little published data exist on these properties, and some of the published results varied significantly. Furthermore, while some manufacturers have independently tested their products, hexagonal mesh is the only fabric type that has a widely accepted, standardized test method (ASTM A 975) in North America to evaluate these properties. Additionally, there is no widely accepted test method to allow for the comparison of engineering properties for a variety of

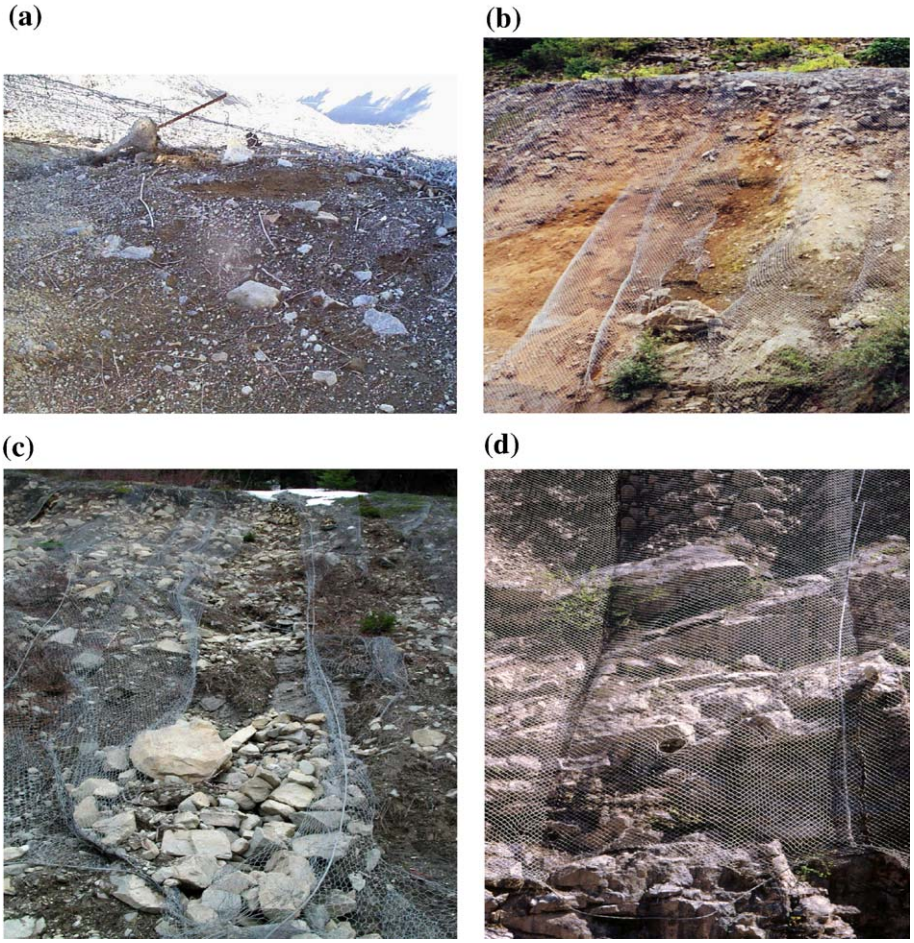

Fig. 2. Illustrative examples of drapery mesh system failure: (a) anchor pullout failure of drapery system; (b) mesh tear due to excessive debris accumulation; (c) rupture of vertical seam and fabric; the mid slope horizontal support cable (d) puncture of the fabric due to rock impact.

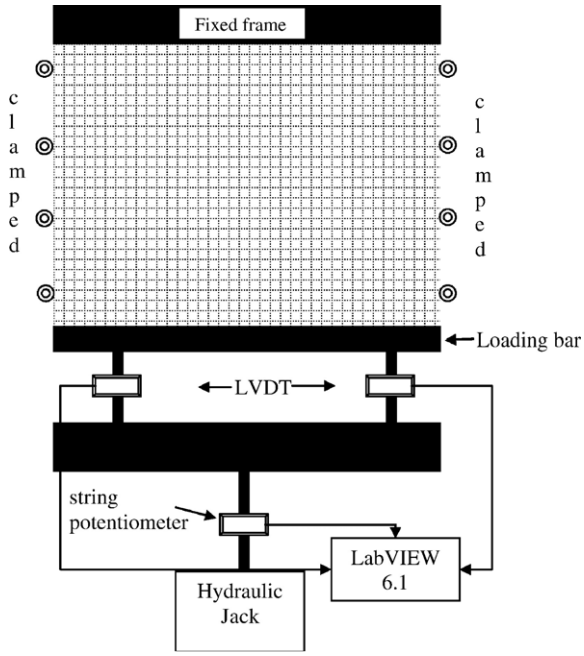

Fig. 3. Schematic diagram of mesh testing arrangement.

fabric types. Therefore, independent tests were conducted at the Wood Materials and Engineering Laboratory (WMEL) at Washington State University in Pullman, Washington.

Fig. 3 shows the schematic of the test fixture that was designed, fabricated and bolted to the reaction floor inside the WMEL's structural testing facility. The intent of the test fixture was to load the fabrics in tension along the longitudinal direction of fabrics while restraining the edges parallel to the direction of loading from constricting as loads were applied. Loads were applied utilizing a 445 kN capacity hydraulic actuator with a stroke of 25.4 cm that was controlled using an MTS 407 Controller, which received actuator displacement feedback using a string potentiometer. Load data were obtained using a 445 kN capacity load cell placed in line with the loading apparatus. Linear variable differential transformers (LVDTs) and string potentiometers were used to monitor displacement of the loading head with respect to the base of the test apparatus in order to get an accurate record of the distance the meshes moved through the first 5 cm of displacement. Load data and displacement data from the string potentiometer and the 2 LVDTs were recorded using LabVIEW version 6.1 software. Differences in dimensions of the meshes made it necessary to make a slight modification of the test apparatus. A detailed account of such modification and other relevant information are provided in a comprehensive report (Muhunthan et al., 2005).

Attachment of the loading plates was done far enough from the ends of the meshes so that the wires would not unwind or come undone prior to failure of the specimens. All specimens were placed in the fixture in such a way that as much slack could be taken out of the specimens as possible. This was done to ensure that there would be enough deformation of the specimens to cause failure. In general there was very little load applied to the specimens as they were installed in the test fixture.

All specimens were secured in the test frame, and then the LVDTs or string potentiometers were installed such that the maximum amount of displacement data could be recorded before the instruments ran out of stroke on the plunger or extension of the string. Following installation of the displacement measuring devices, the data acquisition program was started and the hydraulic actuator was put into action. Load was induced by the hydraulic actuator, which ran at 6.35 mm per minute under displacement control.

Fig. 4 shows the typical load–displacement behavior of Maccaferri double-twisted hexagonal wire mesh, Geobrugg TECCO® wire mesh, and Maccaferri cable net. It can be seen that the behavior of these fabrics can be approximated to be linear elastic until a peak has been reached. Accordingly, Table 1 summarizes the strength and modulus parameters for the finite element analyses obtained from these tests. It is noted that in some cases the strength and modulus values that were obtained from our testing varied from the values reported by the manufacturers. This may be due to

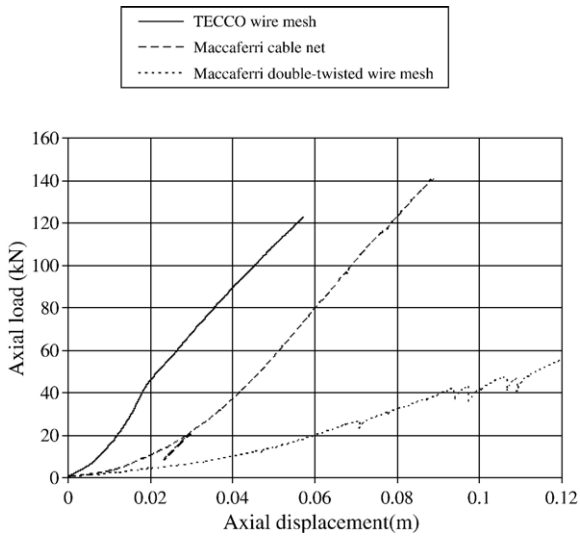

Fig. 4. Typical load–displacement curve for Maccaferri double-twisted, TECCO® wire meshes and Maccaferri cable net.

Table 1
FE model parameters for different meshes

Type	Young's modulus (MPa)	Yield or breaking strength (MPa)
Maccaferri double-twisted mesh	850	15
TECCO® G65 mesh	170	30
Maccaferri cable net	14000	175

differences in the type of tests, specimen size, and the boundary and loading conditions. It is emphasized here that the testing performed for this research was not intended to compare the performance of fabric types from different manufacturers. Rather, the testing enabled us to compare the performance of these systems under a range of modulus and strength values.

3. Finite element model

Finite element analyses were conducted using the computer code ABAQUS (2003). The finite element discretization of the wire mesh system is as shown in Fig. 5. Since the mesh carries the load with its end restraint in a "membrane type" action, the mesh was modeled using a three-dimensional membrane element from the ABAQUS library (ABAQUS, 2003). The top horizontal rope and support ropes were modeled using three-dimensional hybrid beam elements. Hybrid beam element is a special purpose element that is capable of simulating a cable-type structural element. The external support from the anchors is assumed to be pinned. The two vertical edges and the bottom edge are left free as these are not bolted or fixed to the ground in practice. The finite element model was first verified using some field test results (Sasiharan et al., 2005).

4. Interface friction

In all but vertical to overhanging slopes, the interface friction developed between the mesh and the ground surface can be a major contributor to the stability of the wire mesh and cable net systems. The interface friction is controlled by macro and micro roughness of the surface. Macro roughness is the degree of large-scale irregularities of the slope, and micro roughness is related to surface texture. In the case of a smooth planar slope, minimal interface friction may be present, and the mobilized force on the system is carried largely by the anchors. When a slope is highly irregular and the surface is rough or has abrupt protrusions, very high interface friction may be present. In these cases, very little to no mobilized force may be imparted to the anchors. Interface friction is a difficult parameter to quantify in practice. In the absence of either back-calculated values or field measurements, the interface friction angle can be crudely estimated based on observed slope irregularity and surface roughness using the guidelines below. Additional guidance on

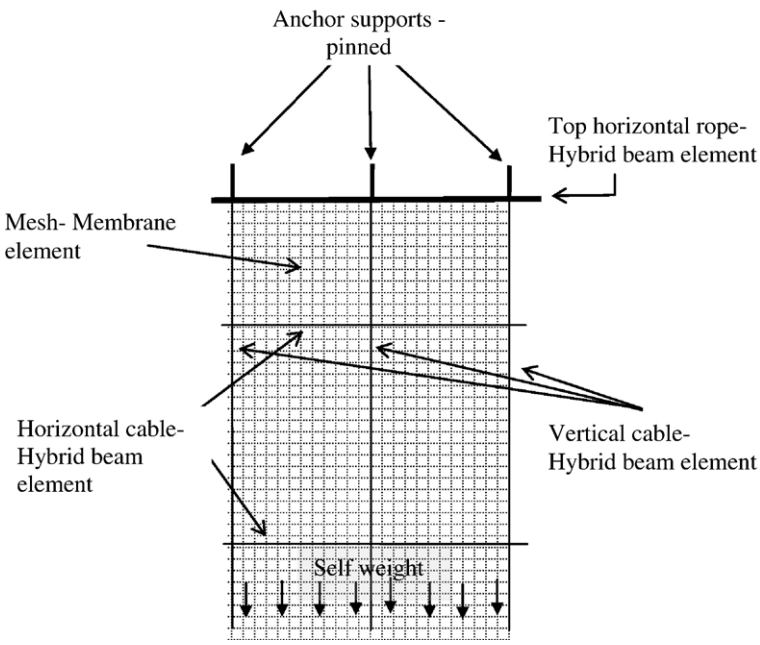

Fig. 5. Finite element model and boundary conditions.

the characterization and verification of the friction angles recommended below are presented elsewhere (Muhunthan et al., 2005).

4.1. Rough slope

The slope surface is very irregular and undulating and has many and/or prominent protrusions on the surface. As a result, both micro and macro roughness contribute to a large effective increase in interface friction. For such cases, the interface friction angle is assumed to be above 60°. For moderate to high degree of mesh contact with the slope, the possibility of global instability of a system on such a slope is very low under normal conditions. Note, however, as slope irregularity and surface roughness increase, mesh contact area usually decreases.

4.2. Undulating slope

The slope is undulating but there are few and/or small abrupt protrusions on the surface. As a result, both micro and macro roughness contribute to an effective increase in the interface friction of the slope. Accordingly, the interface friction angle is assumed to be between 36° and 59°.

4.3. Planar slope

The slope is planar, and the surface is fairly smooth and has few small undulations. In this case, only micro roughness is assumed to contribute to the frictional resistance. Accordingly, the interface friction angle is assumed to be between 25° and 35°.

The values of the interface friction angle proposed above for the rough and undulating slopes were examined and verified by finite element analyses and through limit equilibrium back analyses of existing stable and failed installations. To examine the friction contribution, finite element analyses were carried out with selected internal supports within the mesh region for an assumed 45° slope and the increases in "effective" friction angle were determined. Several iterations were performed by varying the location of the internal support to determine the most critical configuration. For an undulating slope, the location of the internal support was varied whereas for the rough slope two to three internal support points were varied inside the mesh. The reaction loads on anchors with the internal supports were obtained first. Subsequently, the interface friction angle on an equivalent slope with no internal support was varied until the results matched.

5. Element performance in wire mesh and cable net systems

The current practice of wire mesh and cable net protection systems often includes a widely spaced grid of interior horizontal and vertical support ropes throughout the field of the mesh (Fig. 1). However, it has been known through field observations that this practice does not provide significant mechanical benefit (Duffy et al., 2005). Optimizing the design of the system by eliminating some elements in the wire mesh/cable net protection systems could reduce construction costs. Therefore, finite element analyses were consecutively carried out to evaluate the mechanical contribution, if any, of each system element.

First, the installation supported by anchors was analyzed without any horizontal and vertical support ropes (Fig. 5). The resulting von-Mises stress distribution is shown in Fig. 6. Stresses are concentrated around the anchor support and a significant segment of the mesh experiences much lower stress distribution.

Subsequently, the system was assumed to be installed with a top horizontal support rope (Fig. 5). The resulting stress distribution is shown in Fig. 7. The use of a top horizontal rope significantly reduces the maximum stress level around the anchor (5.5 MPa to 3 MPa) by distributing it along the entire length of the support rope (Fig. 7).

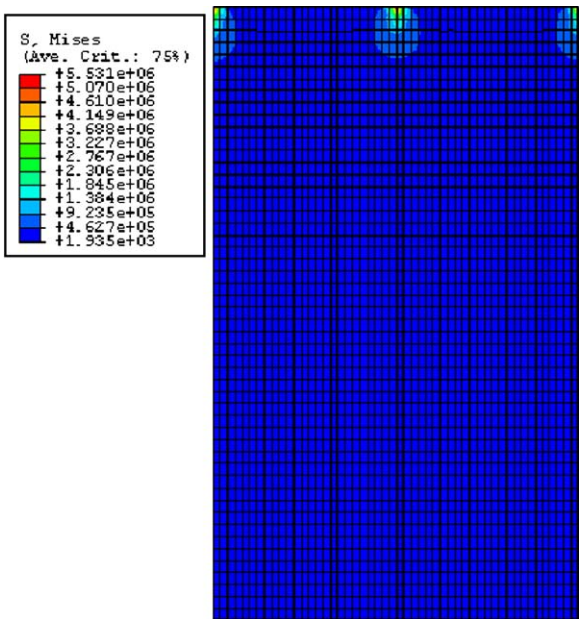

Fig. 6. Von-Mises stress distribution on the mesh (load from mesh weight only).

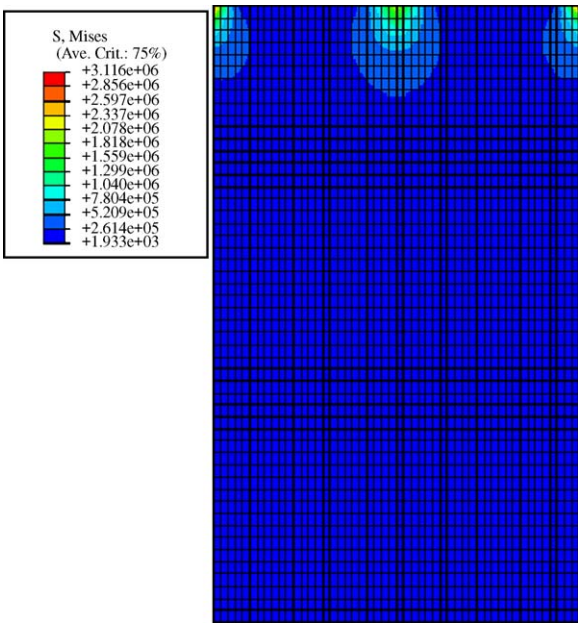

Fig. 7. von-Mises stress distribution on the mesh with top horizontal rope.

The analysis was repeated with the addition of vertical support ropes on the anchor locations (Fig. 8). Their addition nearly eliminated the stress concentration on the mesh around the anchors. The stresses on other segments also dropped significantly. Further, the addition of the vertical rope reduced the stress level in the horizontal rope. Therefore, it is evident that with the use of vertical support ropes the mesh system would remain stable immediately after construction under its own weight. Note that the pattern of the stress distribution was found to be dependent on the ratio of the modulus of the vertical rope and the mesh. When the modulus of the rope and the mesh were nearly the same, the distribution pattern followed that is shown in Fig. 7.

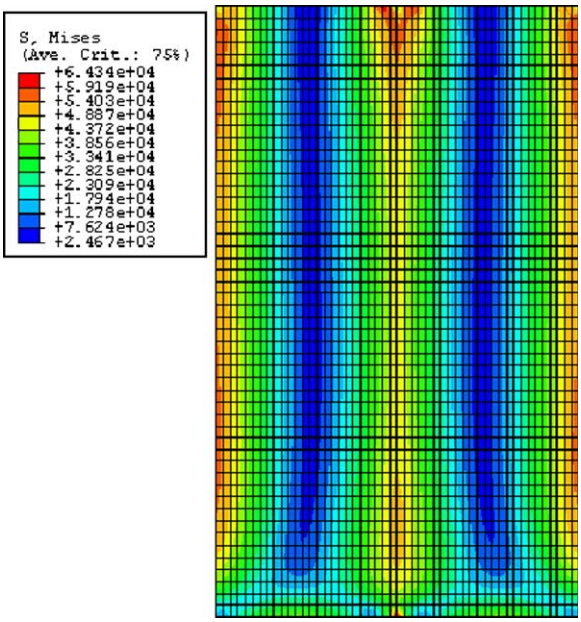

Fig. 8. von-Mises stress distribution on the mesh with top horizontal rope and vertical support ropes.

Analyses were also conducted to study the effectiveness of adding additional interior horizontal support ropes (Fig. 1). However, their addition did not make changes to the stress levels or to the distribution. Therefore, their use in current practice does not have any mechanical benefit (see also Table 2).

The maximum value of the stress experienced by each element for the different cases is shown in Table 2. It can be seen that the maximum stress on the vertical support rope is much smaller than that on the top horizontal support rope. Consequently, the vertical ropes need not be as strong as the top horizontal rope in the design.

In the current practice, where vertical support ropes are included, the mesh is fastened to vertical ropes with lacing wire and does not grip the rope. Hence, there is no vertical load transfer of the mesh weight to the vertical support ropes. Thus, there is no effective mechanical benefit. If the mesh were to be clamped at close spacing to the vertical ropes, the mechanical benefit would potentially be realized up to the localized yield stress of the mesh connection detail.

Table 2
Summary of von-Mises stresses for different support rope arrangements

Arrangement	Description	von-Mises stress (MPa)		
		Mesh	Top horizontal cable	Vertical supporting cable
Arrangement 1	Mesh only (no top horizontal cable and support ropes)	5.60	–	–
Arrangement 2	Mesh with top horizontal rope	3.20	65.0	–
Arrangement 3	Mesh with top horizontal and vertical supporting ropes	.064	12.2	2.48
Arrangement 4	Mesh with top horizontal cable and horizontal supporting ropes	3.20	71.0	–
Arrangement 5	Mesh with top horizontal, vertical and horizontal supporting ropes	.064	11.8	2.03

6. Anchor spacing and anchor load

FE analyses were also carried out to develop design charts for a variety of combinations of slope lengths, fabrics, slope angles, and interface friction. The charts are developed for four slope lengths 15.2, 30.5, 61, and 91.5 m, three types of fabrics, three types of slope surfaces, and for slope angles of 45, 60, and 90°. Fig. 9 shows the variation of anchor load with anchor spacing for three different fabrics. Fig. 10 shows the variation

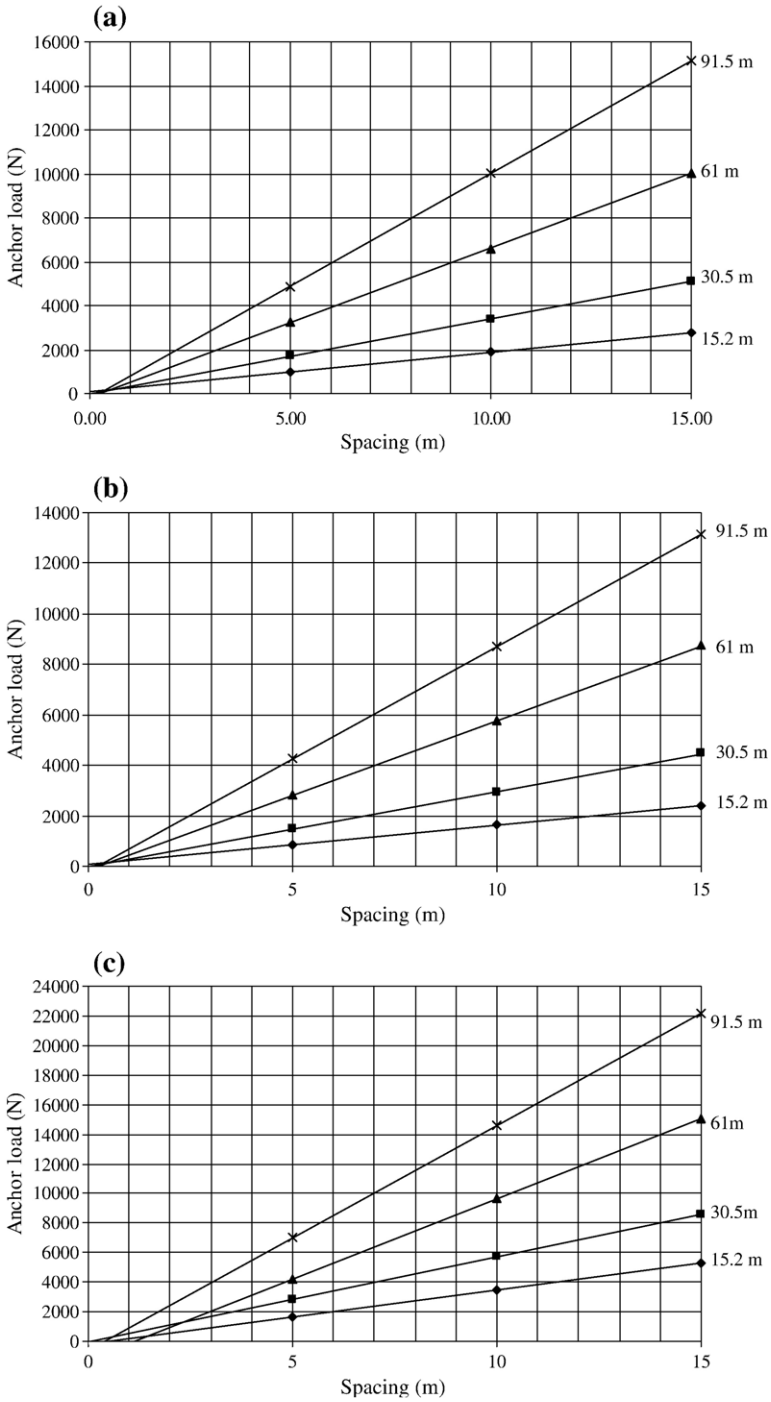

Fig. 9. Variation of anchor load vs. spacing for (a) double-twisted hexagonal wire mesh, (b) TECCO® G65 mesh and (c) cable nets for 60° planar slope.

of anchor load with spacing for different slope surface conditions. The results are for the mesh on a vertical slope without debris load, and the interface friction is absent. Therefore, these values could be considered to provide the most conservative anchor loads for a given spacing. Similar analyses were conducted for a suite of slope and interface friction angles and the results are reported in Muhunthan et al. (2005).

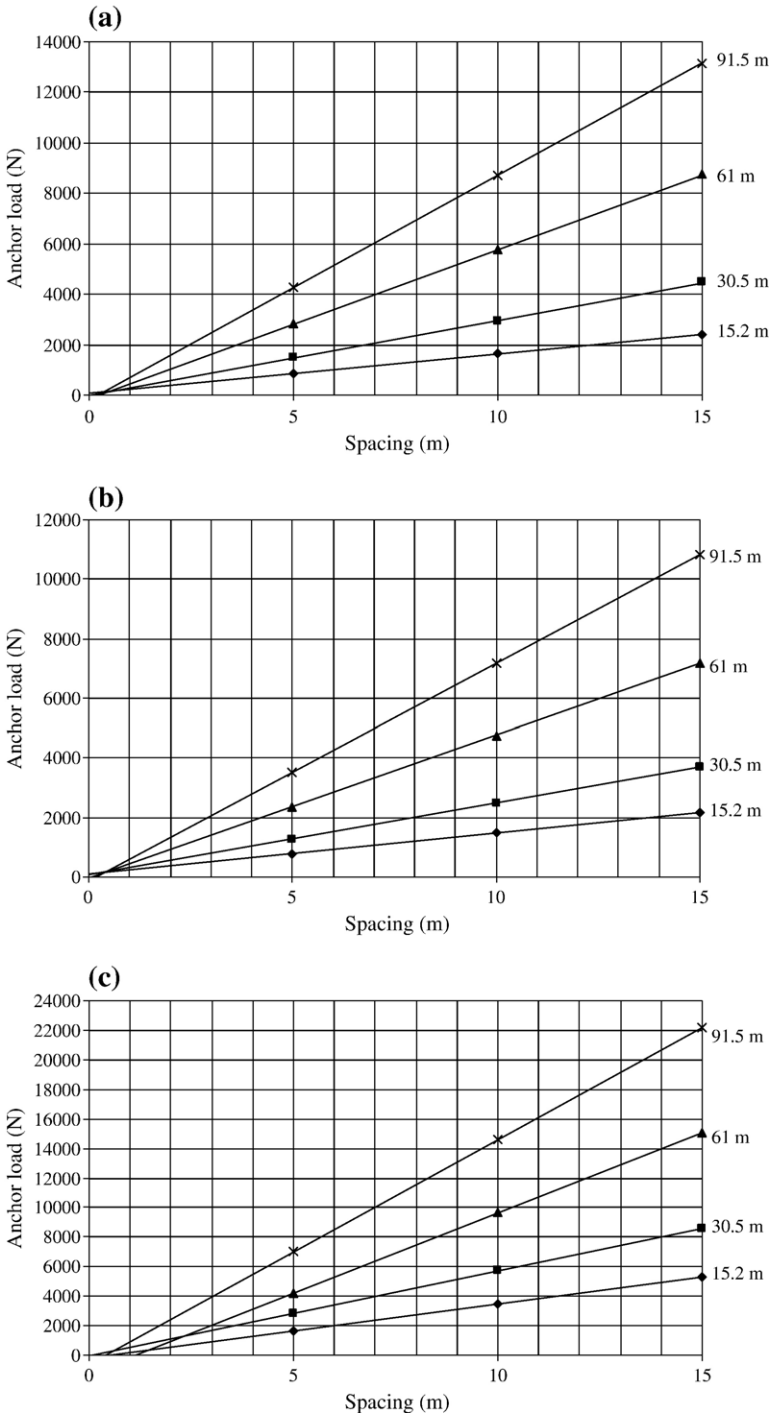

Fig. 10. Variation of anchor load vs. spacing for TECCO® G65 mesh for 60° (a) planar, (b) undulating and (c) rough slopes.

7. Simple design example

Consider the case of a double-twisted wire mesh placed on a 60° planar slope with the height of 22.86 m and anchor spacing of 7.62 m. The anchor spacing was chosen to conform to the current empirical guidelines presented earlier. The analysis of this system gives an anchor load of about 20 kN (Fig. 9(a)). Typical anchors used in North America have the capacity that generally exceeds 90 kN in both tension and shear. Thus, the use of an anchor spacing of 7.62 m results in a factor of safety of 4.5. On the contrary, the use of Fig. 9(a) shows that that the anchor spacing as wide as 15 m could be used on the same slope with the factor of safety of 2. Increasing anchor spacing will reduce the number of anchor, hence the cost of construction. It is noted, however, if other external loads such as snow are present then the design anchor spacing must be reduced. Such considerations are presented elsewhere (Shu et al., 2005; Muhunthan et al., 2005)

8. Limiting conditions on global stability

The FE analyses were also used to determine the maximum height of installation, the maximum debris load for each fabric for different anchor spacing, and the maximum uninterrupted length of the top horizontal rope.

8.1. Maximum installation height

To determine the maximum height of installation for a specific fabric, the analyses used a 90° slope (no interface friction) with a 6 m and 15 m anchor spacing. The three fabrics that were evaluated are as follows:

- a double-twisted hexagonal mesh of galvanized 3 mm diameter wire, (supplied by Maccaferri),

Table 3
Fabrics yield states as function of height

Fabric	Maximum height of installation for 15 m spacing (m)	Maximum height of installation for 6 m spacing (m)
Double-twisted, hexagonal mesh	105–115	<170
TECCO® G65 mesh	135–150	<215
Maccaferri cable net	180–230	<250

Table 4
Fabric yield states as a function of debris load

Fabric	Maximum debris volume that can accumulate between anchors of 15 m spacing	Maximum debris volume that can accumulate between anchors of 6 m spacing
Double-twisted hexagonal mesh	1.9 m^3	1.6 m^3
TECCO® G65	3.7 m^3	2.9 m^3
Maccaferri cable net	5 m^3 [19 m^3]	5.7 m^3 [15 m^3]

- a high tensile steel, TECCO® G65 mesh of corrosion protected 3 mm diameter wire (supplied by Geobrugg), and
- a 300 mm square grid, cable net of 8 mm wire rope diameter (supplied by Geobrugg).

The result for each fabric is shown in Table 3. Note that these yield states are considerably larger than the highest installations of current practice, which approach 125 m in North America.

8.2. Maximum debris load

FE analyses were carried out to determine the maximum debris load for a 45° slope, 30 m slope length with a 6 m and 15 m anchor spacing. It is assumed that a debris load would be distributed uniformly over the entire width. The unit weight of the debris is assumed to be equal to 2100 kg/m^3. Note that the maximum debris load for double-twisted hexagonal mesh and TECCO® G65 mesh was determined by limiting the yield strength of the meshes with an assumed anchor capacity of 90 kN. Since the yield strength of the cable net is much higher, the anchor capacity (90 kN) will be the limiting factor in determining the maximum debris load (Table 4). Assuming that the anchor capacity was not the limiting factor but the cable net is the first to yield, then much higher debris loads can be carried by the cable nets as shown in the bracketed values in Table 4. The corresponding anchor loads for this yield state for a

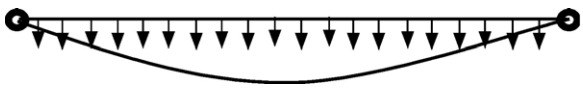

Fig. 11. Load distribution in the top horizontal support rope.

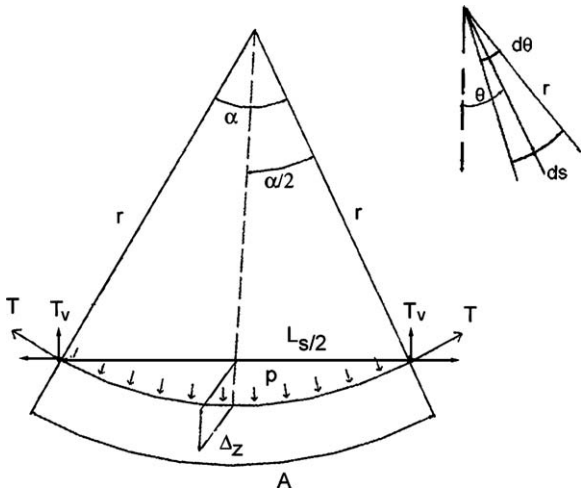

Fig. 12. Schematic diagram of top horizontal cable under mesh load.

15 m and 6 m anchor spacing are 275 kN and 230 kN, respectively.

8.3. Horizontal rope

The top horizontal support rope is a critical structural element in any installation. Fig. 11 shows the typical loading arrangement of a top horizontal support rope. Maximizing the uninterrupted length of the top horizontal rope and, thus, minimizing connections reduces the installation cost of a system. These lengths, however, are limited by their tensile capacity and sag of the rope, and can be calculated by using standard equations for a laterally loaded cable.

The schematic diagram of a circular membrane under a constant pressure p is shown in Fig. 12. For vertical equilibrium:

$$T = p \cdot r \tag{1}$$

where T is the tensile force and r is the radius of the circle.

Let us assume that the length of the mesh segment before deflection is L_s. If the strain ε_y at yielding within this segment is assumed to be uniform, the deformed arc length, A, can be given by:

$$A = L_s(1 + \varepsilon_y) \tag{2}$$

The radius of the circle and the subtended angle α are related by:

$$r = \frac{L_s}{\sin\frac{\alpha}{2}} \tag{3}$$

Table 5
Maximum length for top horizontal support rope for Maccaferri double-twisted mesh

Slope length (m)	Maximum length for 13 mm cable; fabric weight only (m)	Maximum length for 19 mm cable; fabric weight only (m)
15	140	250
30	75	130
60	35	65
90	25	45

Using the Taylor series expansion and approximating an explicit expression, α can be obtained as:

$$\frac{\alpha}{2} = \sqrt{6\left(1 - \frac{L_s}{A}\right)} \tag{4}$$

The maximum deflection at the mid section is,

$$\Delta Z = r\left(l - \cos\frac{\alpha}{2}\right) \tag{5}$$

From above equations, contact pressure p (in this case it would be the uniformly distributed load along the rope) can be calculated as,

$$p = \frac{8T\Delta Z}{L_s^2} \tag{6}$$

Note an iterative procedure should be adopted, as cable weight is a function of the length of the horizontal rope. The calculations were carried out for wire rope sizes that are most typically used in North American installations. The tensile capacities of typical horizontal ropes of 13 mm and 19 mm diameter are approximately 110 kN and 220 kN, respectively. The maximum length of unsupported section of a rope with no interface friction was found for double-twisted hexagonal mesh and TECCO® mesh (Table 5) and cable net backed with double-twisted hexagonal mesh (Table 6). Note that these values are calculated for mesh weight only. If other external loads such as snow or debris contribute then the required lengths will become shorter.

Table 6
Maximum length for top horizontal support rope for Maccaferri double-twisted mesh with Maccaferri cable net backup

Slope length (m)	Maximum length for 13 mm cable; fabric weight only (m)	Maximum length for 19 mm cable; fabric weight only (m)
15	50	90
30	25	45
60	15	25
90	8	15

9. Conclusions

This study presented the results of finite element analyses on the performance of wire mesh systems. It is found that the load–displacement behavior of widely used fabrics can be approximated to be linear elastic until a peak has been reached.

The friction between the mesh and rock is a major contributor to the stability of the wire mesh and cable net systems. The interface friction is controlled by macro and micro roughness of the surface. Interface friction is a difficult parameter to quantify in practice. It is shown that interface friction can be quantified into three major categories: rough, undulating, and planar, based on observed slope irregularity and surface roughness. Based on finite element analyses and confirmed through limit equilibrium back analyses of existing stable and failed installations, the friction angle of a rough slope is estimated to be above 60° and the corresponding ranges for undulating and planar ranged from 36° to 59° and from 25° to 35°, respectively.

The study shows the top horizontal rope to be an essential element in the design. Under the self weight of the mesh as the only external load, the stress concentrations within the mesh and the stress on the top horizontal rope are relatively low. However, if external loads such as snow are present, the use of vertical ropes could reduce stress concentrations around the anchor support by distributing it over the mesh, provided only if the mesh can be securely clamped to the vertical support ropes at close intervals. If such close securement can be accomplished, the analyses show that vertical ropes do not need to be as strong as the top horizontal support ropes. In practice, however, closely spaced clamping of the mesh to vertical support ropes would be costly and time consuming, likely proving to be too costly for the benefit provided. The stiffness of vertical ropes must be much higher than the fabric for distributing the stress. More significantly in terms of reduced installation cost and improved system performance, is the confirmation of field observations through finite element analyses that interior horizontal support ropes within the field of the mesh provide no mechanical benefit for reducing stresses within the mesh.

Design charts for designing anchor spacing for different fabrics are given. Limiting values for maximum installation height, debris volume, and maximum uninterrupted top horizontal rope length were also developed for typical fabrics and tabulated. A suite of comprehensive design charts and consideration of snow and impact loads are presented in Muhunthan et al. (2005).

Acknowledgements

The study was sponsored by the Washington State Department of Transportation with financial contributions from contributory state and provincial DOTs and technical input by the technical advisory committee for this pooled-fund research program. The authors are also grateful to Geobrugg of Sante Fe, New Mexico and Maccaferri of Virginia for providing materials for testing and proprietary test data.

References

ABAQUS: Finite Element Software Package. Hibbitt, Karlsson and Sorrenson, Inc. Version 6.3-1.

Duffy, J., Ingram, H., Badger, T.C., 2005. Personal Communications.

Hearn, G., 1995. Testing and Modeling of Two Rockfall Barriers. . Transportation Research Record. National Research Council, Washington, DC, pp. 1–11.

Hearn, G., Akkaraju, L., 1995. Analysis of cable nets for boulder impacts. ASCE 10th EMD Boulder, CO, pp. 289–292.

Muhunthan, B., Shu, S., Sasiharan, N., Hattamleh, O.A., Badger, T.C., Lowell, S.M., Duffy, J.D., 2005. Analysis and Design of Wire Mesh/Cable Net Slope Protection, Washington State Transportation Center (TRAC) Report No. WA-RD 612.1, Seattle, Washington. 267pp (http://www.wsdot.wa.gov/biz/mats/Geotech/WA-RD612.1WireMesh.pdf).

Pfeiffer, T.J., Higgins, J.D., 1990. Rockfall hazards analysis using the Colorado Rockfall Simulation Program. Transportation Research Record, vol. 1288. TRB, National Research Council, Washington D.C., pp. 117–126.

Ritchie, A.M., 1963. Evaluation of rockfall and its control. Highway Research Record, vol. 17. TRB, National Research Council, Washington D.C., pp. 18–23.

Sandwell Incorporated, 1995. Structural evaluation of slope mesh system, prepared for British Columbia Ministry of Transportation. Sandwell Report, vol. 113576.

Sasiharan, N., Muhunthan, B., Shu, S., Badger, T.C., 2005. Analysis of global stability, anchor spacing, and support cable loads in wire mesh and cable net slope protection systems. Transportation Research Record: Journal of the Transportation Research Board 1913, 205–213.

Shu, S., Muhunthan, B., Badger, T.C., 2005. Snow loads on wiremesh and cable net slope rockfall protection systems. Engineering Geology 81, 15–31.

Smith, D.D., Duffy, J.D., 1990. Field tests and evaluation of rockfall restraining nets. Report No. CA/TA-90/05, California Department of Transportation, Transportation Materials and Research.